Growth and arrest of topological cycles in small physical networks

Timothy W. Sirk[a,1]

[a]Polymers Branch, US Army Research Laboratory, Aberdeen Proving Ground, MD 21005

Edited by Angel Rubio, Max Planck Institute for the Structure and Dynamics of Matter, Hamburg, Germany, and approved June 8, 2020 (received for review April 3, 2020)

The chordless cycle sizes of spatially embedded networks are demonstrated to follow an exponential growth law similar to random graphs if the number of nodes N_x is below a critical value N_*. For covalent polymer networks, increasing the network size, as measured by the number of cross-link nodes, beyond N_* results in a crossover to a new regime in which the characteristic size of the chordless cycles h_* no longer increases. From this result, the onset and intensity of finite-size effects can be predicted from measurement of h_* in large networks. Although such information is largely inaccessible with experiments, the agreement of simulation results from molecular dynamics, Metropolis Monte Carlo, and kinetic Monte Carlo suggests the crossover is a fundamental physical feature which is insensitive to the details of the network generation. These results show random graphs as a promising model to capture structural differences in confined physical networks.

spatial network | thermoset | polymer topology

Physical interaction networks are a central concept in the characterization of disordered materials. Examples from materials science span van der Waals networks in glasses (1), hydrogen bond percolation (2), contact networks in jamming and glass transition (3, 4), and transient networks (5) such as polymer entanglements (6). Such materials are often found in confined environments where the equation of state differs strongly from the bulk behavior, such as those networks confined in holes, slabs, and films, and on periodic surfaces. For polymers in particular, links are well established between the connectivity of polymer chains and the physical properties of the bulk material. The design of new polymer network structures to exploit topological differences is undoubtedly a rapidly emerging area (7), and recent progress in the characterization of bulk materials has been made through network disassembly spectroscopy (8), nuclear magnetic resonance spectroscopy (9), and analytical work to predict the elasticity of gels and elastomers (e.g., see ref. 10). Nonetheless, experiments have, so far, been unable to characterize the network structure in the general terms of graph theory, and the most accessible features involve low-order cycles that strongly influence rubber elasticity, such as loops composed of one or two molecules.

Here, a systematic study of finite-size networks from simulations is presented, where we consider covalent polymer networks as representative spatial networks with intermediate order. Compared with random networks, introducing spatial (e.g., polymer chains) or chemical (covalent network junctions) constraints has the effect of lowering the number of accessible topological states and the corresponding measures of entropy (11). In what follows, a crossover is identified between two regimes, one consisting of small random-like networks that are seemingly unaffected by the spatial constraints of the polymer chains and the other consisting of larger networks having the structure of the bulk material. An analogy of the structure of small physical and random networks is explored, where the structural measure is taken as the mesh size of the network, that is, the size of cycles without a bisecting chord.

Results and Discussion

A number of simulation methods have been used to model the covalent structure of polymer networks, both with and without explicit spatial embedding. These include kinetic Monte Carlo (12–14) (kMC), graph-driven statistical models (15, 16), Metropolis Monte Carlo (17, 18) (MMC), and molecular dynamics (MD). In this work, end-linking polymer networks were generated with a quenched MMC approach, which creates a spatially embedded network by assigning edges that have a small length in Cartesian distance and simultaneously satisfy the chemical constraints of the polymer chains and cross-linker molecules. That is, a regular network is created where edges (polymer chains) are assigned to nodes (cross-linker molecules) such that each node has the same degree (covalent bonds per molecule) of f_x. An example snippet of a polymer network is shown in Fig. 1*A*. The influence of finite-size effects was then studied with a series of simulations where the number of nodes N_x is varied from 50 to 5,000. The values of f_x and N_x were independently varied, while the number of edges was fixed as $N_x f_x/2$ to maintain a stoichiometric mixture of polymer chains and cross-linker molecules. The size of the simulation cell was scaled to maintain a constant monomer density of $\rho = 0.85$ for all simulations. Five independent replicas of each f_x–N_x pair were created, and the chordless cycles were determined for each network. Reference calculations with kMC and MD were carried out to verify the MMC predictions. For further comparison, random networks were generated with similar values of f_x–N_x, in which the only constraints were a regular distribution of the node degree. For all networks, we take the maximum of the distribution of chordless cycle sizes as a characteristic mesh size h_* (19) and study the relationship of h_* with N_x. (See *Materials and Methods* for details.)

The mesh size of random and polymer networks is shown in Fig. 1*B* for f_x in the range of three to eight (20). For small values of N_x, both types of networks are seen to follow an exponential law of the form $N_x(h_*) = \alpha\beta^{h*}$, where the parameters α and β depend strongly on the node degree f_x. Increasing f_x leads to a rapid decrease of h_*, which is consistent with analytical predictions for other measures of shortest cycles in random networks (21). As N_x increases, the physical constraints of the polymer networks enforce a crossover to the bulk behavior in which h_* reaches a plateau value at y_* and the corresponding number of nodes N_*. Increasing N_x beyond N_* does not change the mesh size. The mesh size distributions corresponding to the arrest of h_* are shown in Fig. 1*B*, *Insets*, where each curve is found for

Author contributions: T.W.S. designed research, performed research, analyzed data, and wrote the paper.

The author declares no competing interest.

Data deposition: Supporting data and procedures can be accessed at Figshare (DOI:10.6084/m9.figshare.12276626).

[1]Email: timothy.w.sirk.civ@mail.mil.

First published June 22, 2020.

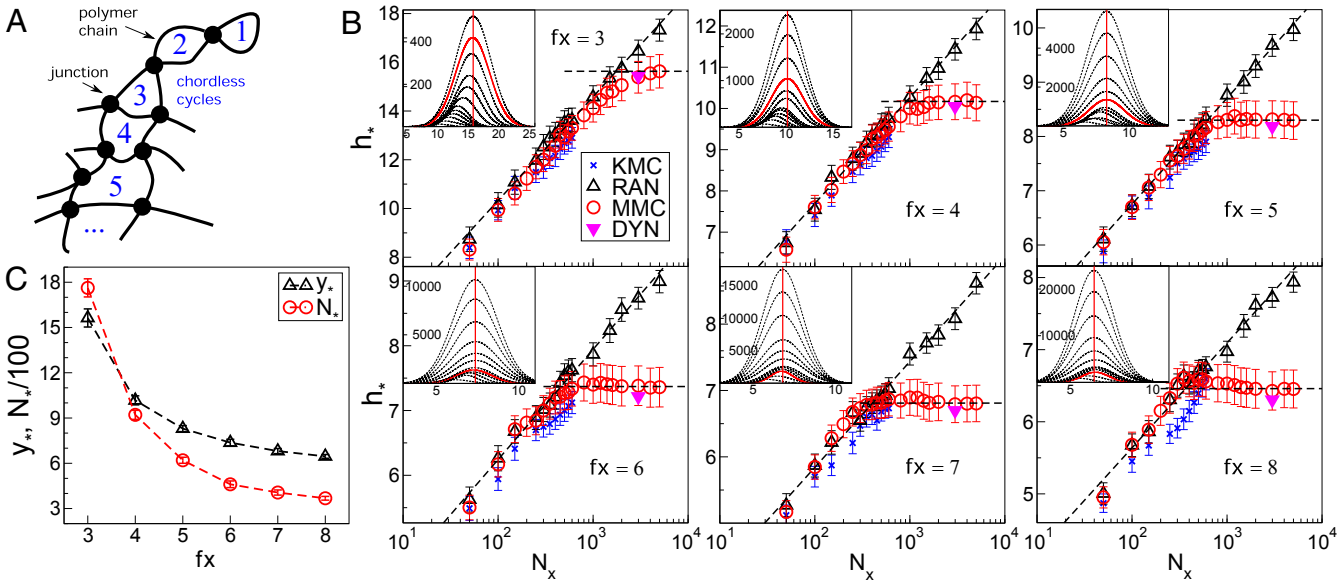

Fig. 1. Summary of high-order chordless cycles found in polymer networks. (*A*) The structure of polymer networks. (*B*) Relationship of the characteristic cycle size h_* and the number of cross-linkers N_x for random (RAN) networks, MMC, kMC (KMC), and dynamic simulations (DYN). Numerical fits of random networks to $N_x(h_*) = \alpha\beta^{h}*$ and $h_* = y_*$ are shown (dashed lines) for $f_x = 3 - 8$. (*Insets*) Approximate mesh size distributions, where each curve is taken as a Gaussian fit to five MMC simulations of size N_x. The distribution corresponding to N_* and the characteristic mesh size y_* are shown in red. (*C*) Relationship of the junction functionality f_x with the crossover cycle size y_* and the corresponding number of nodes N_*.

one value of N_x; the relations of f_x with y_* and N_* are shown in Fig. 1*C*.

Importantly, correlations can be established between the bulk mesh size y_* with the number of nodes at the crossover N_* as well as the parameters of the exponential law (α and β). This connection is widely useful, as it allows the presence of finite-size effects to be predicted from the number of nodes in the physical network, a quantity that can be estimated from experiments. Further, the intensity of the finite-size effect (for those networks with $N_x < N_*$) can be understood by treating the small physical network with the exponential law given above for random networks. As demonstrated in Fig. 2, both N_* and parameters α and β are related to y_* through a power law dependence. For the regular spatial nets considered here, the minimal number of nodes to capture the bulk structure is in the range of about 400 to 16,000, depending on the bulk mesh size, and follows a power law of the form $N_* \approx y_*^c$ with $c \approx 1.70$.

In the case of polymer networks, the effect of a related measure of chordless cycle size, the smallest loop size, has been shown analytically and numerically as a negative correction (e.g., see ref. 22) to the elastic modulus. In other materials, the nature of the physical constraints can be expected to change the details of the finite-size behavior, particularly if the mesh size or other topological features cannot be reduced in size due to chemical considerations such as unfavorable bond angles, steric hindrance, or chain stiffness. Nonetheless, the result given here suggests that descriptions of random networks, like those given in Fig. 2, can incorporate confinement effects into equations of state or constitutive laws that explicitly include the topological structure of the forces. Thus, continued work in this area has potential for a broad analogy of small physical and random networks that informs material properties under confinement.

Materials and Methods

Simulation Details. Polymer networks use the usual freely jointed bead–spring model for polymer chains with Langevin dynamics described by Kremer and Grest (23). The beads of each linear chain interact through the truncated shifted Lennard-Jones potential $U_{LJ}(r) = 4\varepsilon[(\sigma/r)^{12} - (\sigma/r)^6 - (\sigma/r_c)^{12} + (\sigma/r_c)^6]$, where ε and σ are chosen as unity, and the force cutoff r_c is $2^{1/6}$. All bonds were represented with the finite extensible nonlinear elastic (FENE) potential, $U_{FENE}(r) = (-KR_0^2/2)\ln[1 - (r/R_0)^2]$, with $R_0 = 1.5\sigma$ and $K = 30\varepsilon\sigma^2$. Each system was created with a self-avoiding random walk of monodisperse chains of length $N = 32$ mixed with a stoichiometric number of single cross-linker beads at a density of $\rho = 0.85$. The systems were then equilibrated with dynamics under periodic boundary conditions for $10^4\tau + 1{,}000N^2\tau$ with a time step of 0.005τ. The chain ends form, at most, one new bond ($f_m = 2$), while each cross-linker bead can form a bond with as many as f_x linear chains, where f_x is varied from three to eight. These systems correspond to cross-link densities, taken as $2\rho/(Nf_x)$, in the range of $0.0066\sigma^{-3}$ to $0.0177\sigma^{-3}$, where σ is the monomer size. The system size was varied by creating a series of 21 networks with values of cross-linker number N_x spanning the range 50 to 5,000 and a corresponding number of beads ranging from 2,450 to 645,000. The ratio of the edge length of the simulation cell to the chain radius of gyration was between 5 and 40 for all networks. (24).

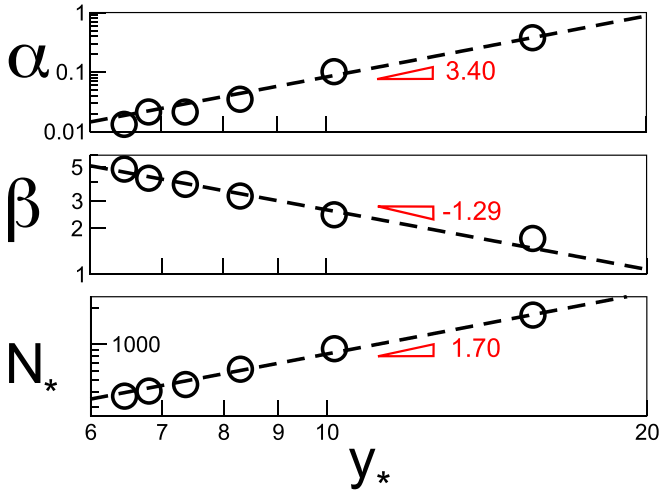

Fig. 2. Relation of the parameters α (*Top*) and β (*Middle*) to the bulk mesh size y_*. The minimal number of nodes N_* needed to converge the network to the bulk mesh size, as a function of the bulk mesh size (*Bottom*).

Simulation Methods.

Random networks. The method of Steger and Wormald (25) was used to generate networks with a uniform degree d equal to the cross-linker functionality. 1) A network of N_x nodes is created with no edges. 2) A list of unique pairs of nodes is created and maintained such that the degree of any node is at most $d-1$. 3) A pair of nodes u,v is selected from the list with probability proportional to $(d-d(u))(d-d(v))$. 4) The edge is added to the network. 5) Steps 1 to 4 are repeated until all nodes have the same degree d.

Simulated annealing optimization. A tempered MMC optimization was used to generate network structures (18). Stoichiometric mixtures of N_x cross-linkers and N_l linear chains were relaxed at constant volume with a density of 0.85. The network connectivity was then assigned using the simulated annealing method, which minimizes the total length of the newly created bonds. Bond swap and bond translation moves were considered. Both moves were accepted with probability taken from a harmonic energy penalty, $P(\Delta L) = \min[\exp(-\Delta L^2), 1]$. No other restrictions were considered. Five independent structures with different network connectivity were prepared for each pair of $f_x - N_x$.

Other reference calculations. A rejection-free kMC algorithm was adapted from recent work of Wang et al. (14). The algorithm checks the probability of closing a chain between cross-linker molecules under the assumption of Gaussian behavior, including self-connections.

Dynamics. Networks were grown with reactive, dynamic simulations based on local bonding rules. The bonding rule was chosen strictly such that cross-link bonds are created only if reactive monomers directly contact one another, that is, the collision cross-section is chosen as a fixed value of $R = 2^{1/6}\sigma$ (26, 27). A stoichiometric mixture of N_m chains and N_x cross-linker beads was distributed in the simulation box; the mixture was equilibrated well above the glass transition temperature at $T = 1.0\varepsilon/k_B$; cross-link bonds were formed during dynamics when the reactive sites approached within $2^{1/6}\sigma$ until the system reached 97.7% cure. All dynamic simulations used the Large-scale Atomic/Molecular Massively Parallel Simulator package (28).

Cycle counting. Chordless cycles were taken as a closed walk on nonrepeating nodes in which no interior edges serve as a shorter chord connecting two nodes of the cycle. The identified chordless cycles are identical to the irreducible shortest path rings identified by Matsumoto et al. (29). In practice, this was carried out by recording, for each node, the shortest paths between all pairs of the node neighbors that are closed without a chord, up to a cutoff distance varied between 10 and 25 edges. Redundant instances of the same cycle were eliminated with homology tests, resulting in a single record of each chordless cycle and its size h. Self-loops and second-order cycles were directly counted as $h = 1$ and 2, respectively. Multiple edges were considered as follows: A node i with one or more repeating edges N_e to a neighboring node creates at least one second-order cycle, where the number of induced cycles is related to the number of redundant edges as $N_{2,i} = \binom{N_e}{2}$. For cycles of order three or more, any second-order cycles internal to the main cycle were treated as a single edge. Supporting data and procedures can be accessed at http://doi.org/10.6084/m9.figshare.12276626.

ACKNOWLEDGMENTS. I thank Robert M. Elder, Berend C. Rinderspacher, and Randy Y. Mrozek for useful discussions. The US government is authorized to reproduce and distribute reprints for government purposes notwithstanding any copyright notation hereon.

1. S. V. King, Ring configurations in a random network model of vitreous silica. *Nature* **213**, 1112–1113 (1967).
2. M. Z. Brela, P. Kubisiak, A. Eilmes, Understanding the structure of the hydrogen bond network and its influence on vibrational spectra in a prototypical aprotic ionic liquid. *J. Phys. Chem. B* **122**, 9527–9537 (2018).
3. A. Zaccone, E. M. Terentjev, Disorder-assisted melting and the glass transition in amorphous solids. *Phys. Rev. Lett.* **110**, 178002 (2013).
4. H. A. Vinutha, S. Sastry, Force networks and jamming in shear-deformed sphere packings. *Phys. Rev.* **99**, 012123 (2019).
5. J. Billen, M. Wilson, A. Rabinovitch, A. R. C. Baljon, Topological changes at the gel transition of a reversible polymeric network. *EPL* **87**, 68003 (2009).
6. S. Jabbari-Farouji, O. Lame, M. Perez, J. Rottler, J.-L. Barrat, Role of the intercrystalline tie chains network in the mechanical response of semicrystalline polymers. *Phys. Rev. Lett.* **118**, 217802 (2017).
7. Y. Gu, J. Zhao, J. A. Johnson, A (macro) molecular-level understanding of polymer network topology. *Trends Chem.* **1**, 318–334 (2019).
8. H. Zhou *et al.*, Counting primary loops in polymer gels. *Proc. Natl. Acad. Sci. U.S.A.* **109**, 19119–19124 (2012).
9. K. Saalwächter, S. Seiffert, Dynamics-based assessment of nanoscopic polymer-network mesh structures and their defects. *Soft Matter* **14**, 1976–1991 (2018).
10. R. Wang, A. Alexander-Katz, J. A. Johnson, B. D. Olsen, Universal cyclic topology in polymer networks. *Phys. Rev. Lett.* **116**, 188302 (2016).
11. K. Anand, G. Bianconi, Entropy measures for networks: Toward an information theory of complex topologies. *Phys. Rev.* **80**, 045102 (2009).
12. J. Mikes, K. Dusek, Simulation of polymer network formation by the Monte Carlo method. *Macromolecules* **15**, 93–99 (1982).
13. S. Dutton, R. F. T. Stepto, D. J. R. Taylor, Monte-Carlo modelling of the formation, structure and properties of polymer networks. *Die Angew. Makromol. Chem.: Appl. Macromol. Chem. Phys. Angew Makromol. Chem.* **240**, 39–57 (1996).
14. R. Wang, T.-S. Lin, J. A. Johnson, B. D. Olsen, Kinetic Monte Carlo simulation for quantification of the gel point of polymer networks. *ACS Macro Lett.* **6**, 1414–1419 (2017).
15. M. Lang, W. Michalke, S. Kreitmeier, A statistical model for the length distribution of meshes in a polymer network. *J. Chem. Phys.* **114**, 7627–7632 (2001).
16. W. Michalke, M. Lang, S. Kreitmeier, D. Göritz, Comparison of topological properties between end-linked and statistically cross-linked polymer networks. *J. Chem. Phys.* **117**, 6300–6307 (2002).
17. S. Kirkpatrick, C. D. Gelatt, M. P. Vecchi, Optimization by simulated annealing. *Science* **220**, 671–680 (1983).
18. R. Khare, M. E. Paulaitis, S. R. Lustig, Generation of glass structures for molecular simulations of polymers containing large monomer units: Application to polystyrene. *Macromolecules* **26**, 7203–7209 (1993).
19. H. D. Rozenfeld, J. E. Kirk, E. M. Bollt, D. Ben-Avraham, Statistics of cycles: How loopy is your network?*J. Phys. Math. Gen.* **38**, 4589–4595 (2005).
20. T. Sirk, Cycle data for "Growth and arrest of topological cycles in small physical networks." Figshare. Dataset, https://doi.org/10.6084/m9.figshare.12276626.v1. Deposited 18 May 2020.
21. H. Bonneau, A. Hassid, O. Biham, R. Kühn, E. Katzav, Distribution of shortest cycle lengths in random networks. *Phys. Rev.* **96**, 062307 (2017).
22. M. Lang, Elasticity of phantom model networks with cyclic defects. *ACS Macro Lett.* **7**, 536–539 (2018).
23. K. Kremer, G. S. Grest, Dynamics of entangled linear polymer melts: A molecular-dynamics simulation. *J. Chem. Phys.* **92**, 5057–5086 (1990).
24. B. Dünweg, K. Kremer, Molecular dynamics simulation of a polymer chain in solution. *J. Chem. Phys.* **99**, 6983–6997 (1993).
25. A. Steger, N. C. Wormald, Generating random regular graphs quickly. *Combinator. Probab. Comput.* **8**, 377–396 (1999).
26. E. R. Duering, K. Kremer, G. S. Grest, Structure and relaxation of end-linked polymer networks. *J. Chem. Phys.* **101**, 8169–8192 (1994).
27. C. Jang, T. W. Sirk, J. W. Andzelm, C. F. Abrams, Comparison of crosslinking algorithms in molecular dynamics simulation of thermosetting polymers. *Macromol. Theory Simul.* **24**, 260–270 (2015).
28. S. Plimpton, Fast parallel algorithms for short-range molecular dynamics. *J. Comput. Phys.* **117**, 1–19 (1995).
29. M. Matsumoto, A. Baba, I. Ohmine, Topological building blocks of hydrogen bond network in water. *J. Chem. Phys.* **127**, 134504 (2007).